




## Green Synthesis of Silver Nanoparticles Decorated With Exfoliated Graphite Nanocomposites

Asia Abdul Waheed Daood<sup>1</sup>, Ahmed Ali Moosa<sup>1\*</sup>, Muhammed Mizher Radhi<sup>2</sup>

<sup>1</sup>Technical Engineering College-Baghdad, Middle Technical University, Baghdad, (MTU) Iraq. 

<sup>2</sup>Radiological Techniques Department, Health and Medical Technology College-Baghdad, Middle Technical University, Baghdad, (MTU) Iraq;

### Abstract

Silver nanoparticles (AgNPs) were prepared by a rapid, simple, and economic microwave assisted synthetic route using aqueous spent black tea leaves extract and silver nitrate solution. The exfoliated graphite (EG) was rapidly and efficiently prepared from natural graphite using domestic microwave oven. Natural graphite powder was hand mixed with  $\text{KMnO}_4$  and  $\text{HNO}_3$  at a weight ratio of 1:1:2 for 5 min to produce graphite intercalation compound (GIC). The GIC was then washed and dried at 110 °C for 6 hrs. The Exfoliated graphite (EG) was prepared by rapid heating of graphite intercalation compound (GIC) in a domestic microwave oven at power of 540 and 700 W for 60sec. Silver nanoparticles was then loaded on the exfoliated graphite to obtain exfoliated graphite decorated with silver nanoparticles nanocomposite (EG/AgNPs). The prepared materials were characterized by ultraviolet–visible spectrophotometry, X-ray diffraction (XRD), Fourier transform infrared spectroscopy (FT-IR), and scanning electron microscopy (SEM). The prepared EG/AgNPs nanocomposites showed uniform dispersion of Ag nanoparticles on the surface of expanded graphite with little agglomeration.

**Keywords:** Silver nanoparticles, GICs, exfoliated graphite, Ag-EG nanocomposites

### 1. Introduction

Graphite is composed of many layers of graphene. The bond strength within the graphene layers is much higher than perpendicular to them and this difference in bond strength accounts for the anisotropic properties of graphite [1]. One of the outcomes of such anisotropy in graphite is the ease of inserting molecular layers of a different chemical substance called the intercalates between graphene layers to form graphite intercalation compounds (GICs) such as graphite bisulfate and graphite nitrate [2]. The graphite intercalation compound is also called expandable graphite since it can be exfoliated upon heating [3]. In a potassium-GIC, the intercalation process increases the spacing between the graphene layers from 0.34 nm to 0.53 nm [4]. The increased distance between the layers in the GIC leads to the weakening of the van der Waals attraction between the graphene layers. Rapid heating of the intercalated graphite makes graphite expand dozens or even hundreds of times along the C axis, which is perpendicular to the crystal basal planes, due to the sudden vaporization or decomposition of intercalating species. This is called the exfoliation process, which gives exfoliated graphite (EG) [5, 6]. Graphite intercalated compound (GIC), also called expandable graphite, and is prepared by inserting of

chemical ions between the layers of bulk graphite [7]. Exfoliated graphite, also known as expanded graphite [7], is prepared usually by brutal heating of GIC using a preheated tubular furnace, laser irradiation, and microwave (MW) irradiation [8, 9]. Microwave-assisted exfoliation of graphite is considered efficient and a quick approach to preparing EG because it can be performed at room temperature in a few minutes in a simple laboratory facility [9, 10, 11]. This process is accompanied by lightning and fuming. Microwave irradiation gives a higher expansion volume than the conventional heating method using an electrical furnace at a temperature of over 1000°C [9]. EG has a worm-shaped, accordion-like material with a porous cellular structure, low bulk density, a large specific surface area, high lubricity, high flexibility, and high-temperature resistance [11]. Exfoliated graphite can be rolled into flexible graphite without any binder to produce foils or sheets with different thicknesses and densities [7]. It can be compacted into gaskets and can be used as composite materials [12]. EG is a porous material consisting of a small thickness of stacks of graphene sheets (20–70 nm) with a high concentration of nanopores (2–5) nm in size [13]. The exfoliated graphite can be used in various applications, such as electrode materials, adsorbents, heat-resistant materials, and sealing materials [8]. EG is a good

\*Corresponding author e-mail: [ahmeda1752@yahoo.com](mailto:ahmeda1752@yahoo.com)

. Receive Date: 27 May 2022, Revise Date: 27 June 2022, Accept Date: 13 July 2022

DOI: 10.21608/EJCHEM.2022.141183.6180

©2022 National Information and Documentation Center (NIDOC)

carbon-support material for metallic nanoparticles, due to its porous structure, a worm-shaped material, large specific surface area, low cost, and good resistance to both acidic and basic environments [14, 15].

Silver nanoparticles (AgNPs) have good unique physicochemical and biological properties, such as high electrical and thermal conductivity, chemical stability, high catalytic activity, and superior antibacterial activity [16]. Many studies have demonstrated the successful preparation of AgNPs using different methods. The green synthesis of AgNPs using plant extracts and waste plant products is an attractive method that is low cost and less likely to contaminate the final products [17]. Various plant extracts have been utilized to synthesize silver nanoparticles, such as *Justicia adhatoda* plant extract [Lohithan et al., 2020] [16]; Egyptian propolis extract as reducing and capping agent [18]; Fruit extract [19]; Aloe Vera plant extract [20a]; spent tea leaves extract [20b]; *Ziziphus* plant [21]; *Conyza canadensis* leaf extract [22]. In this study, EG decorated with silver nanoparticles (EG/AgNPs) was prepared and evaluated. EG was prepared by microwave irradiation of GIC, while AgNPs were prepared by reduction of AgNO<sub>3</sub> using tea leaves extract. The aim of this work is to prepare exfoliated graphite (EG) materials by microwave irradiation of the graphite intercalation compound (GIC) as a quick and energy-saving approach. Also, in the present study, we reported a green method for synthesizing AgNPs using spent black tea leaves extract as a low-cost, simple, and microwave-assisted green method. Silver nanoparticles (AgNPs) were then loaded onto the exfoliated graphite to produce a silver nanoparticle-exfoliated graphite nanocomposite (AgNPs-EG). The prepared materials have been characterized on the basis of UV-Vis, FT-IR, XRD, and SEM.

## 2. Experimental

### 2.1. Materials

Natural graphite powder (99% purity), nitric acid (HNO<sub>3</sub>, 69%, CDH, India), potassium permanganate (KMnO<sub>4</sub>, purity 99%, Merck, Germany), silver nitrate (AgNO<sub>3</sub>, 99% purity, Daejung Chemical & Metal Co., Korea), black tea leaves were purchased from local Iraqi market and the spent black tea leaves were collected from home.

### 2.2. Experimental Methods

#### 2.2.1 Exfoliated Graphite Preparation

Natural graphite powder (99% purity) was sieved and screened by laboratory test sieves (BS 410-1, Endecott's Ltd, England) with different particle sizes 45, 80, 106, 125, 180, 212, 250, and 350 μm. The exfoliated graphite was prepared following the procedures used by [9] and our previous work [23]. The graphite powder sample, KMnO<sub>4</sub>, and HNO<sub>3</sub>

were mixed by a glass rod in a Pyrex glass jar with a weight ratio (graphite: KMnO<sub>4</sub>:HNO<sub>3</sub> = 1:1:2) at room temperature for 5 min. Potassium permanganate (KMnO<sub>4</sub>) was used as an oxidant and nitric acid (HNO<sub>3</sub>) as an intercalation agent (Wei et al., 2008) [9,23]. The mixture is called Graphite Intercalation Compound (GIC) which was then washed several times using vacuum filtration until the pH reached 7 and then dried in a drying furnace at 110 °C for 6 hrs [23]. The exfoliated graphite (EG) was prepared by placing the GIC in a domestic microwave oven (SMB177C6B-P, Bruck, Deutschland) at a power of 540 and 700 W for 60 sec. After microwave irradiation, the pyrex glass jar was cooled down, and the EG was collected for further experimentation. The graphite exfoliation process is accompanied by lightening, fuming, and gas formation [9, 23].

The starting graphite powder and the exfoliated graphite are shown in Figure 1. The exfoliation ratio (expansion ratio) of each sample was calculated as the ratio of exfoliated graphite volume (V<sub>EG</sub>) and EG mass (m). The exfoliation ratio has a unit of volume/mass (mL/g). 0.2 g EG was transferred into a graduated cylinder (50 mL) to measure the volume. Three independent measurements were taken and the average of V<sub>EG</sub> was calculated. The expansion ratio was calculated from Equation 1 [24]:

$$\text{Exfoliation Ratio} = V_{\text{EG}}/m \quad (1)$$

Where m= Mass of exfoliated graphite (0.2 g)

V<sub>EG</sub> = exfoliated graphite volume (mL).

#### 2.2.2. Preparation of Silver Nitrate Solution

Silver nitrate (AgNO<sub>3</sub>, 99% purity, Daejung Chemical & Metal Co., Korea) was used for the synthesis of AgNPs. A 0.213 g of AgNO<sub>3</sub> was added to 250 mL of distilled water in a 500 mL flask to obtain a 5 mM colorless solution of AgNO<sub>3</sub>. The solution was then mixed using a hand mixer and stored in an amber-colored bottle so that auto-oxidation of silver is prevented [19].

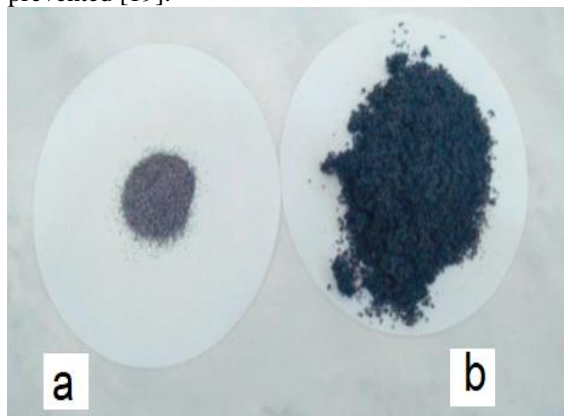


Figure 1. (a) Graphite powder; (b) Exfoliated graphite.

### 2.2.3. Preparation of Spent Black Tea Leaves Extract.

The spent black tea leaves were collected from used tea at home. The tea leaves were washed with distilled water, dried at room temperature, and then stored to be used later. A 10 g of dried spent tea leaves was boiled with 100 mL of distilled water at 80 °C for 5 minutes in a 250 mL flask and then filtered to obtain yellow-brown spent black tea leaves extract [20b].

### 2.2.4. Silver Nanoparticles Synthesis.

For the production of AgNPs, 30 mL of spent black tea leaves extract solution was added to 270 mL of 5 mM silver nitrate aqueous solution in a 500 mL glass flask. The mixture was hand-mixed thoroughly and covered with aluminum foil. The tea leaves extract with silver nitrate mixed solution was then microwave irradiated at a power of 700 W and a frequency of 2.45 GHz for different microwave irradiation times (10, 20, 30, 40, 50, 60, 70, and 80 sec). The color of the mixed solution was changed from yellow-brown to dark brown, indicating the biosynthesis of AgNPs, as shown in Figure 2.

### 2.2.5. Preparation of EG/ AgNPs

After preparing the exfoliated graphite and silver nanoparticles solution, the EG/AgNPs nanocomposites were prepared by adding 1 g from the exfoliated graphite to 250 mL AgNPs [25]. The mixture was hand mixed with a glass rod and then placed into a shaker water bath for 160 rpm and 3 hrs at 60 °C in the dark (covered with aluminum foil with holes made on the surface of the flask to evaporate water). The product solution was filtered and then dried at 80 °C to remove residual water to obtain EG/AgNPs powder.

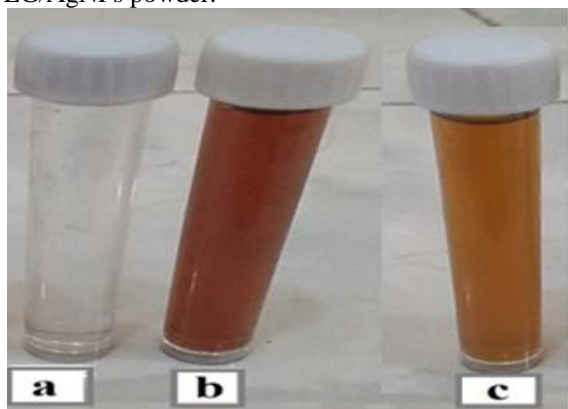


Figure 2. (a) Silver nitrate solution (b) Spent black tea leaves extract solution; (c) silver nanoparticles.

## 3. Characterization

A series of techniques were used to characterize the synthesis of EG/AgNPs. The synthesis of AgNPs was monitored visually by the change in color due to the reduction of  $\text{Ag}^+$  and with the use of ultraviolet-visible (UV-vis) spectrophotometry (UV-Vis, Perkin Elmer, Lambda 365) over the range from 190 to 1100 nm at

room temperature with 0.5 nm as wavelength resolution. Fourier-transform infrared (FTIR) Spectroscopy (Perkin Elmer, Spectrum Two N™, USA) was used to identify the functional groups in the prepared materials. X-ray diffraction analysis (XRD) was used to identify the crystal structure of the graphite, the exfoliated graphite, AgNPs, and EG/AgNPs using (DX-2700B, Dandong Haoyuan, China) at 30Kv, 20 mA with Cu  $K\alpha$  radiation ( $\lambda = 0.15418$  nm), at a scanning rate of 10°/min with angle in the range 10- 80°. Scanning electron microscopy (VP-FeScan, Tescan MIRA3 XMU, Brno, Czech Koruna) was used to get information about the surface topography, and particle size of the graphite, and EG with a resolution of 1-2 nm at an operating voltage of 10 kV.

## 4. Results and Discussion

### 4.1. Effect of Graphite Particle Size on Expanded Volume.

The effect of microwave power on the exfoliated volume of EG using different particle sizes of graphite 45, 80, 106, 125, 180, 212, 250, and 350  $\mu\text{m}$  is shown in Figure 3. The expansion volume of EG increases with the increase of graphite particle size up to 250 microns and then starts to decrease. At microwave power 540 W, the expansion volume is lower than that at 700 W because the energy was not enough for exfoliation processes. The best expansion volume is 120 ml/g at 700 W for graphite particle sizes of 250 microns. During the preparation of EG from GIC by microwave irradiation, the intercalated species between graphite layers vaporize and hence a significant expansion of the material occurs and a low-density exfoliated graphite (EG) is obtained [1].

The expansion volume of EG prepared from graphite flakes with different flake sizes decreased as the particle size of the graphite decreased. For small graphite particle size, the intercalate gas molecules can escape very fast and this prevents the creation of enough pressure required to expand the adjacent graphene layers and results in a low expansion ratio [14, 27]. The same finding was reported and the expansion volume of EG prepared from graphite flakes with different flake sizes (300 and 50  $\mu\text{m}$ ) decreased as the particle size of graphite decreased [26].

### 4.2. X-Ray Diffraction (XRD) Analysis

#### 4.2.1. X-Ray Diffraction (XRD) of Graphite

X-ray diffraction analysis (XRD) was used to investigate graphite, GIC, and EG structures using the Shimadzu diffractometer (Shimadzu XRD-6000, Japan) using Cu  $K\alpha$  radiation ( $\lambda = 0.15418$  nm), 40Kv, 30 mA at a scanning rate of 10°/min with the angle in the range 20- 80°. The diffraction pattern for graphite, Figure 4, has two peaks at 26.68° and 54.88° with the inter-planar crystal spacing of 0.334 and 0.167 nm

respectively corresponding to diffraction planes of (002) and (004).

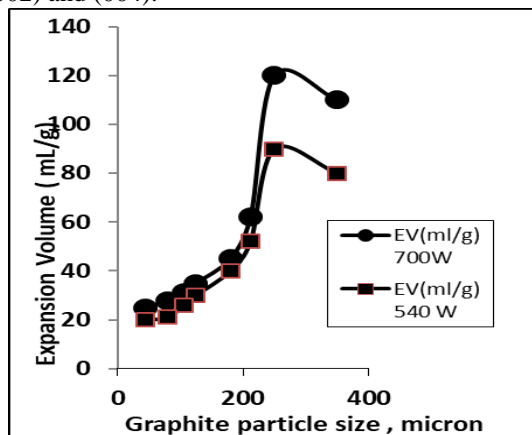


Figure 3. Expansion volume of EG at microwave.

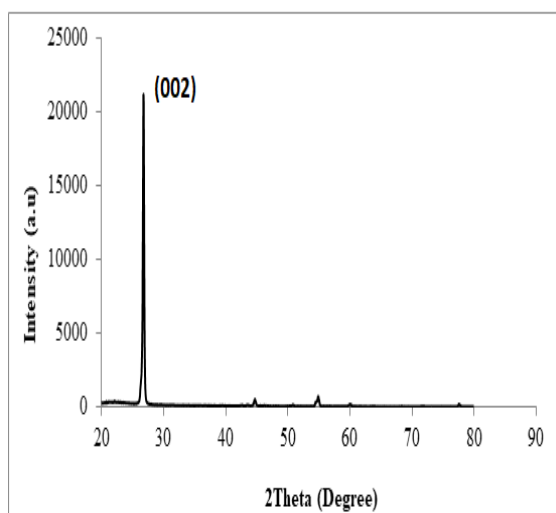


Figure 4. XRD of graphite

#### 4.2.2. X-Ray Diffraction (XRD) for GIC

Figure 5 indicates the (002) peak for the GICs at  $2\theta = 25.114^\circ$  corresponding to a spacing of 0.354 nm. The XRD indicated a broadened (002) peak for GIC compared with that of graphite. The (002) peak for GIC is shifted to a lower angle of  $2\theta = 25.114^\circ$  due to the fact that  $\text{KMnO}_4$  is a strong oxidant, and the graphite layers can be easily oxidized, therefore resulting in the increase in the interlayer spacing due to the increase in the repulsion interactions between the layers. Therefore, the intercalates migrate between the graphite layers and cause the expansion along the *c*-axis direction. Thus, the insertion of intercalates between the graphite layers acts as a defect and hence, the peak intensity of GIC is lower than that of natural graphite [28].

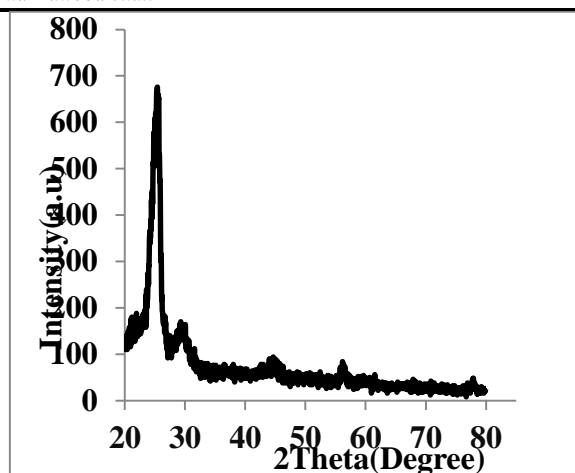


Figure 5. XRD of GIC.

The distance between the graphite layers changed from 0.334 nm in graphite to 0.354 nm in GIC. The (002) peak is broadened in the GIC compared to that of pure graphite. The fact that the (002) peak exists in all graphite products (graphite, GIC, and EG) indicates that the crystal structure of natural graphite is partially conserved and is not undermined by oxidation and intercalation. Potassium permanganate ( $\text{KMnO}_4$ ) as an oxidant has the ability to oxidize and open the graphite layers, and the intercalating agent  $\text{HNO}_3$  could easily move between graphite layers to form GIC, thereby resulting in an increase in the interlayer spacing. Other peaks are observed for the XRD pattern of GIC at  $2\theta = 29.42^\circ$ ,  $44.7^\circ$ , and  $56.28^\circ$ . At  $2\theta = 29.42^\circ$ , the peak is due to the oxidizing and intercalating process. The same results were obtained during the preparation of exfoliated graphite at low temperatures with perchloric acid, phosphoric acid, and  $\text{KMnO}_4$  [29]. The occurrence of sharp peaks at  $2\theta = 26.68^\circ$  in graphite and at  $2\theta = 25.114^\circ$  in GIC suggest that the oxidizing–intercalating process in GIC preparation does not change the layered structure of the flake graphite but only the distance between the layers change slightly. In natural graphite, the reflection peak at  $2\theta = 54.88^\circ$  was shifted to  $2\theta = 56.28^\circ$  in GIC due to the little change in the surface structure of the GIC.

#### 4.2.3. X-Ray Diffraction (XRD) for EG

The XRD pattern of the exfoliated graphite shows two diffraction peaks at  $2\theta = 26.46^\circ$  and  $54.62^\circ$ , as shown in Figure 6. These two peaks correspond to the (002) and (004) planes, respectively. The  $2\theta = 26.46^\circ$  of the exfoliated graphite corresponding to the *d*-spacing of 0.3365 nm decreased in its intensity and broadened in its width in comparison with the natural graphite. In EG, the 002 distance (0.3365 nm) was slightly increased due to the intercalation process, but still kept the planar stacking structure. The

crystallinity of EG is still comparable to that of natural graphite but there is a decrease in the intensity of the reflection peak at  $2\theta = 26.46^\circ$  for EG due to the fact that during microwave irradiation, the intercalation agents expand and there is a pressure exerted by accumulating gas in spaces between the layers [30].

#### 4.3. Scanning Electron Microscopy (SEM) Analysis of Natural Graphite and Exfoliated Graphite.

The surface of the graphite and the exfoliated graphite (EG) were analyzed by scanning electron microscopy (SEM) (TESCAN, Czech Koruna). SEM images indicate a noticeable increase in volume and a difference in the structure between graphite and EG. The graphite flake has a particle size of about 250 microns with a flat and uniform surface, as shown in Figure 7a. Under microwave irradiation, the GICs expand rapidly along the c-axis, resulting in worm-shaped exfoliated graphite, as seen in Figure 7 b. The exfoliated graphite is indicating the well-known cellular microstructure, as shown in Figure 7 c with many pore networks. The pore structures stretched perfectly on the surface of the exfoliated graphite with different sizes and shapes. At a higher magnification of 5000x, the pore size is between 3-5  $\mu\text{m}$ . The exfoliated graphite has a multilayer structure with many diamond-shaped pores.

#### 4.4. UV –Visible Spectral Analysis for AgNPs

Silver nanoparticles (AgNPs) were prepared using 10 mL spent tea leaves extract with 90 mL of  $\text{AgNO}_3$  aqueous solution (5 mM) at different microwave irradiation exposure time (10, 20, 30, 40, 50, 60, and 70) sec. The variation of absorbance with microwave exposure time was recorded using a UV-Vis spectrophotometer (LAMBDA 365, USA) in the wavelength range of 320–850 nm. The color change of  $\text{AgNO}_3$  with spent tea leaves extract solution from yellow-brown to dark brown after microwave irradiation indicates the formation of Ag nanoparticles in the solution [21].

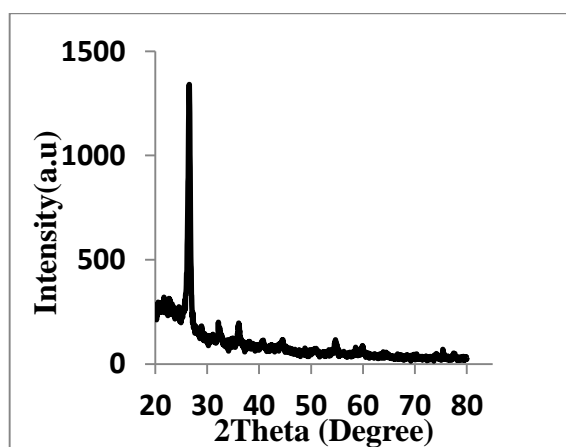


Figure 6. XRD of EG.

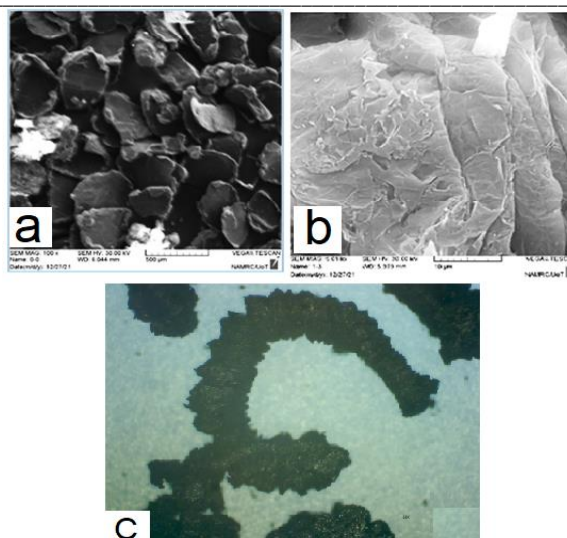


Figure 7. Scanning electron microscopy of (a) graphite; (b) exfoliated graphite, (c) Optical microscope photo of exfoliated graphite (5X).

The reduction of  $\text{Ag}^+$  ions into AgNPs was monitored by recording the absorption spectrum of the reaction mixture with microwave irradiation time. The formation of dark brown color is due to the excitation of surface plasmonic oscillations in the AgNPs [31] which occur in the range of 380 to 440 nm in an aqueous solution [32]. After a series of trials, the best microwave exposure time was selected to be 40 sec based on the absorbance as shown in Figure 8.

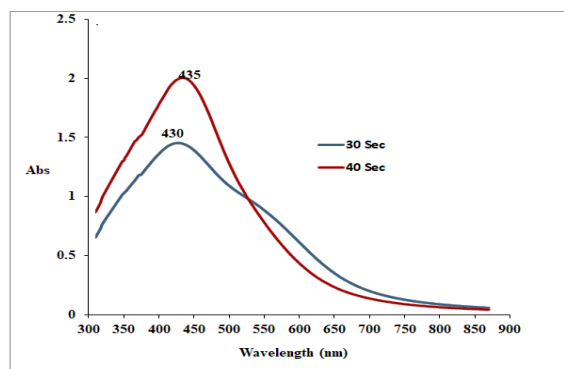
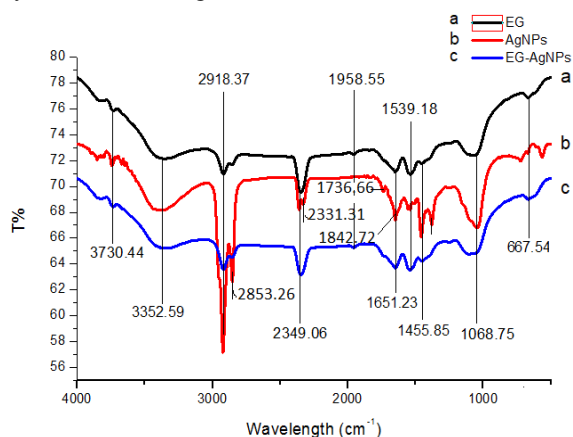


Figure 8. UV spectra of AgNPs at different microwave radiation time (30 and 40 sec).

Throughout this work, the AgNPs were prepared under microwave irradiation for 40 sec. The silver surface Plasmon resonance band occurs at 435 nm for 30 sec and at 430 nm for 40 sec microwave irradiation. These two absorption bands 430 and 435 nm are a typical Plasmon resonance band of silver nanoparticles and the best reduction of silver ions is after 40 sec of microwave irradiation. UV–Vis absorption spectrum indicated there is an almost symmetrical single peak and there are no other peaks located at 335 and 560 nm indicating the absence of nanoparticle aggregation [33].

#### 4.5. Fourier Transform Infrared Spectrophotometer (FTIR)

FTIR analysis was conducted in the range of 4000 to 500  $\text{cm}^{-1}$  to identify the potential functional groups and the bio-molecules in the spent black tea leaves extract which are responsible for the reduction of silver ions into silver nanoparticles ( $\text{Ag}^0$ ). The FTIR analysis of EG, Ag, and EG-Ag are shown in Figure 9. For exfoliated graphite (EG) the peaks are 3730.44, 3352.59, 2918.37, 2349.06, 1958.55, 1651.23, 1539.18, 1455.85, 1068.75, and 667.54  $\text{cm}^{-1}$ . The peak of 3730.44  $\text{cm}^{-1}$  [34] is associated with stretch-free (OH). The peak at 3352.59  $\text{cm}^{-1}$  indicated the presence of -OH. The peaks at 2918.37  $\text{cm}^{-1}$  are ascribed to the aliphatic C-H group [35, 36]. The peak at 2349.06,  $\text{cm}^{-1}$  was observed and attributed to the vibration of C-O [34]. The peak at 1651.23  $\text{cm}^{-1}$  is related to the role of the amide I group [35]. The peak at 1539.18  $\text{cm}^{-1}$  is attributed to secondary amine groups [36]. The peak of 1455.85  $\text{cm}^{-1}$  is related to the symmetric bending of  $\text{CH}_3$  [36].



**Figure 9.** FTIR spectra of : (a)EG ; (b) AgNPs ; and (c) EG-AgNPs.

The band at 1068.75  $\text{cm}^{-1}$  is attributed to C-O stretching vibrations [37]. The peak at 667.54  $\text{cm}^{-1}$  corresponds to the C-H stretching of alkenes [38]. An obvious change in the absorption bands of the functional groups were observed in the spectrum of the Ag (Figure 9 b) with the appearance of new peaks at 3851.35, 3671.01, 3646.8, 2853.26, 2331.31, 1842.72, 1736.66, 1380.62, 723.58, and 669.25  $\text{cm}^{-1}$ . The peak of 3851.35  $\text{cm}^{-1}$  [34] is associated with stretch-free (OH). The band 3671.01  $\text{cm}^{-1}$  is related to alcohol, phenol O-H, and the free group [39]. The peak at 2922.34  $\text{cm}^{-1}$  in FTIR for Ag is very sharp, with a shoulder peak at 2853.26  $\text{cm}^{-1}$  which is ascribed to the aliphatic C-H group [35-36]. These functional groups are involved in the formation of silver nanoparticles [35]. The peak at 2331.31  $\text{cm}^{-1}$  was attributed to the N-H stretching of the secondary amine groups. The peak at 1736.66  $\text{cm}^{-1}$  corresponds to the C=O groups [37]. The peaks 1457.87 and 1380.62  $\text{cm}^{-1}$  are both related to the symmetric bending of

$\text{CH}_3$  [36]. The peak observed at 723.58  $\text{cm}^{-1}$  corresponds to the C-H stretching of alkenes [38]. Thus, the preparation of AgNPs from tea leaves extracts is encompassed by organic materials having functional groups of amines, alcohols, ketones, aldehydes, and carboxylic acids [40]. FTIR analysis reveals that the participation of functional groups like carboxylic acids, proteins, and polyphenols present in the tea leaves extract was responsible for the bio-reduction of silver ions into nanosilver particles [41]. The absorption bands of the functional groups were seen in the FTIR spectrum of the EG-AgNPs (Figure 9c) with the appearance of new peaks at 3819.89, 2854.86, 1103.06  $\text{cm}^{-1}$ . The peak 3819.89  $\text{cm}^{-1}$  [34] is associated with stretch-free (OH). The band in EG at 1068.75 was shifted to 1103.06  $\text{cm}^{-1}$  and is attributed to C-O stretching vibration [37].

#### 4.6. Particle size of the AgNPs

The particle size of the AgNPs was analyzed using a particle size analyzer (Brookhaven 90Plus Nanoparticle Size Analyzer, Brookhaven Instruments Corporation New York, USA). The average size of the synthesized silver nanoparticles from the tea leaves extract was found to be 64.7 nm.

#### 4.7. X-Ray Diffraction (XRD) for AgNPs and EG/AgNPs

The crystallinity of the prepared AgNPs was studied using X-Ray diffraction (XRD). The XRD pattern of AgNPs was recorded using (Dandong Haoyuan DX-2700B, China) with Cu K $\alpha$  radiation ( $\lambda = 0.15418$  nm) operated at 30Kv, 30 mA at a scanning rate of 10 $^\circ$ /min with the angle in the range 10- 80 $^\circ$ . Figure 10 indicates XRD for AgNPs which was prepared using the spent tea leaves extract by microwave irradiation for 40 sec. Four peaks have been observed at 2 $\theta$  values of 38.215, 44.124, 64.483, and 77.361 degrees corresponding to the reflections of (hkl) values - (111), (200), (220), and (311) planes of crystalline silver, respectively. All the observed four diffraction peaks are in good agreement with the standard powder diffraction card of JCPDS, silver file No. 04-0783 [42] as shown in Table 1. The XRD results clearly show that these peaks of the Ag nanoparticles synthesized by the tea leaves extract are matched with the face-centered cubic structure of silver. In addition to these four peaks of FCC silver particles, additional unassigned peaks were observed (marked with circles), Figure 10. These peaks at 32.41, 46.42, 54.20, and 57.40 degrees are due to the unreduced  $\text{AgNO}_3$  that remained in the prepared AgNPs sample in minute quantity. These peaks are not included in Table 1. Similar results were obtained during the preparation of AgNPs by the reduction of silver ions from  $\text{AgNO}_3$  to Ag using fruit extract [43].

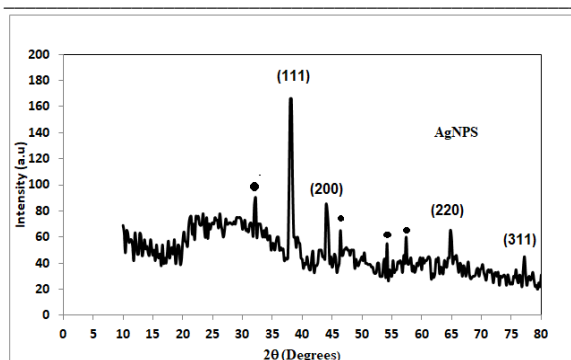


**Figure 10.** XRD of AgNPs

The observation of these peaks also suggests the presence of a crystalline phase of some bio-organic compounds in the preparation of AgNPs using *Coleus aromaticus* leaf extract [44] and also in the preparation of AgNPs using geranium leaves extract [45]. It is clear from the XRD analysis that the silver nanoparticles could be synthesized by reducing silver nitrate with tea leaves extract and the produced AgNPs are crystalline in nature.

**Table 1** Experimental and standard diffraction angles of AgNPs.

Experimental diffraction angle ( $2\theta$ in degrees)	Standard diffraction angle ( $2\theta$ in degrees) JCPDS silver: 04-0783
38.215	38.117
44.124	44.279
64.483	64.428
77.361	77.475

The XRD analysis of the exfoliated graphite (EG) decorated with silver nanoparticles (AgNPs) is shown in Figure 11. The XRD spectrum of EG/AgNPs indicated five characteristic diffraction peaks. The diffraction peak observed at  $2\theta$  value of 26.62 degrees corresponds to the reflection of the (002) plane of graphite. The other four XRD peaks are clearly observed at  $2\theta$  values of 38.215, 44.124, 64.483, and 77.361 degrees. These peaks are corresponding respectively (JCPDS card, No. 04-0783) to the reflections of (hkl) values - (111), (200), (220), and (311) planes of crystalline face-centered cubic silver particles. Thus, the XRD spectrum shows that the expanded graphite was successfully decorated with colloidal AgNPs.

#### 4.8. SEM of EG Decorated with AgNPs

After the preparation of the exfoliated graphite and silver nanoparticles, the silver nanoparticles were loaded on the exfoliated graphite using a shaker water bath at 160 rpm for 3 hrs at 60 °C in the dark, then the solution was filtered and then dried at 80 °C to remove

residual water to obtain EG/AgNPs nanocomposites. SEM images (SEM, MERLIN Compact, Carl Zeiss, Jena, Germany) of EG decorated with AgNPs are shown in Figure 12 at different magnifications. Figure 12a (Mag.: 1KX) indicates AgNPs are well distributed on the EG surface. It is clear that AgNPs are located at the edges and pores of the exfoliated graphite, as shown in Figures 12 (b) and (c). At higher magnification (50KX), SEM shows that the average particle size of AgNPs is close to that measured by the particle size analyzer (64.7 nm). Some agglomeration of AgNPs was also observed.

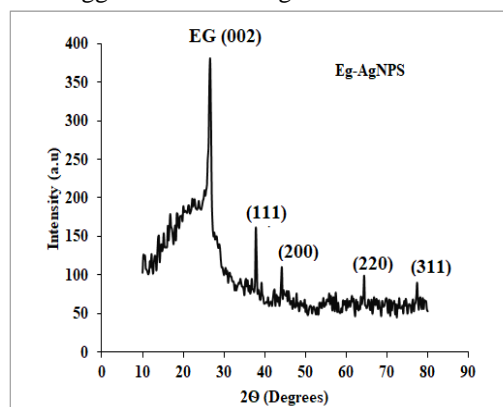


**Figure 11.** XRD of Eg-AgNPs

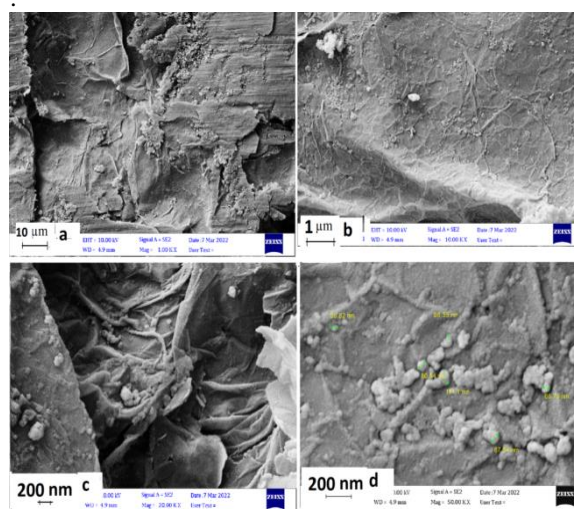


**Figure 12** (a) AgNPs are well distributed on EG surface (Mag.: 1KX); (b) AgNPs are located at the edges and pores of the exfoliated graphite (10KX); (c) 20KX; (d) Higher magnification (50KX).

#### 5. Conclusions

Silver nanoparticles were successfully prepared through the reduction of  $\text{AgNO}_3$  using spent tea leaves extract by microwave irradiation at power 700 W for 40 sec. This method of synthesis of AgNPs is an efficient, environmental ecofriendly and cost effective route. The average AgNPs size is 64.7 nm. A simple and fast route was used to prepare the exfoliated graphite (EG) by MW irradiation of the GIC compound using a combination of graphite:  $\text{KMnO}_4$ :

HNO<sub>3</sub> at a mixing ratio of 1:1:2. The best exfoliation ratio was obtained at maximum MW irradiation power of 700 W and a frequency of 2.45 GHz for 60 sec. The AgNPs was then decorated with EG by adding 1g from the exfoliated graphite to 250 mL AgNPs using shaker water bath for 160 rpm, 3 hrs. at 60 °C in the dark to obtain EG/AgNPs. SEM showed that AgNPs are well dispersed and strongly attached to the edges and the functional groups of the EG surface.

## References

- 1- A. Celzard, J. Marech, G. Furdin, "Modelling of exfoliated graphite", *Progress in Materials Science*, vol. 50, no.1, pp. 93-179, 2005. Available: [10.1016/j.pmatsci.2004.01.001](https://doi.org/10.1016/j.pmatsci.2004.01.001).
- 2- M. Inagaki, "Applications of graphite intercalation compounds", *Journal of Materials Research*, vol. 4, no. 6, pp. 1560-1568, 1989. Available: [10.1557/JMR.1989.1560](https://doi.org/10.1557/JMR.1989.1560)
- 3-D. Chung, "A review of exfoliated graphite", *Journal of Materials Science*, vol. 51, pp.554-568, 2015. DOI: [10.1007/s10853-015-9284-6](https://doi.org/10.1007/s10853-015-9284-6)
- 4- M. Dresselhaus, G. Dresselhaus, "Intercalation compounds of graphite", *Advances in Physics*, vol.51, no.1, pp.1-186, 1981. DOI: [10.1080/00018738100101367](https://doi.org/10.1080/00018738100101367)
- 5-S.H. Anderson, D.D.L. Chung, " Exfoliation of intercalated graphite", *Carbon*, vol. 22, no. 3, pp. 253-263, 1984. [https://doi.org/10.1016/0008-6223\(84\)90169-6](https://doi.org/10.1016/0008-6223(84)90169-6).
- 6- X. Wang, G. Wang, L. Zhang, "Green and simple production of graphite intercalation compound used sodium bicarbonate as intercalation agent", *BMC Chemistry*, vol.16, no.1, p.13, 2022. <https://doi.org/10.1186/s13065-022-00808-y>.
- 7- E. Solfiti and F. Berto, "Mechanical properties of flexible graphite: review", *Procedia Structural Integrity*, vol. 25, pp. 420-429, 2020. <https://doi.org/10.1016/j.prostr.2020.04.047>.
- 8-D. Chung, "Exfoliation of graphite", *Journal of Materials Science*, vol. 22, no.12, pp.4190-4198, 1987. Available: [10.1007/bf01132008](https://doi.org/10.1007/bf01132008).
- 9-T.Wei, Z.Fan, G.Luo, C. Zheng and D.Xie, "A rapid and efficient method to prepare exfoliated graphite by microwave irradiation", *Carbon*, vol.47, no.1, pp. 337-339, 2009. Available: [10.1016/j.carbon.2008.10.013](https://doi.org/10.1016/j.carbon.2008.10.013).
- 10- O.Y.Kwon, S.W.Choi, K.W. Park , Y.B.Kwon, "The preparation of exfoliated graphite by using microwave", *Journal of Industrial and Engineering Chemistry*, vol.9, no.6, 743-747, November, 2003.
10. Kwon OY., Choi SW., Park KW., Kwon,YB. "The preparation of exfoliated graphite by using microwave". *Journal of Industrial and Engineering Chemistry*, 9(6), 743-747(2003).
- 11- J. Kim, S. Oh, H. Kim, B. Kim, K. Jeon, and S. Yoon, "Expanding characteristics of graphite in microwave-assisted exfoliation", *Sci. Coop. Int. Work. Eng. Branches*, vol.1, pp. 273–277, 2014.
- 12- A. Yakovlev, A. Finaenov, S. Zabud'kov and E. Yakovleva, "Thermally expanded graphite: Synthesis, properties, and prospects for use", *Russian Journal of Applied Chemistry*, vol. 79, no. 11, pp. 1741-1751, 2006. <https://doi.org/10.1134/S1070427206110012>
- 13- V. Ogenko, L. Dubrovina, O. Naboka and I. Dubrovin, "Exfoliated graphite modified with pyrolytic carbon", *Inorganic Materials*, vol. 50, no. 4, pp. 344-348, 2014. <https://doi.org/10.1134/S002016851404013X>
- 14- Ö. Çalm, A. Kurt and Y. Çelik, "Influence of expansion conditions and precursor flake size on porous structure of expanded graphite", *Fullerenes, Nanotubes and Carbon Nanostructures*, vol.28, no.8, pp.611-620, 2020. Available: [10.1080/1536383x.2020.1726894](https://doi.org/10.1080/1536383x.2020.1726894).
15. S. Park, J. Kim, K. Jeon and S. Yoon, "Characterization on the Expanding Nature of Graphite in Microwave-Irradiated Exfoliation", *Journal of Nanoscience and Nanotechnology*, vol. 16, no. 5, pp. 4450-4455, 2016. Available: [10.1166/jnn.2016.10980](https://doi.org/10.1166/jnn.2016.10980).
16. R. Lohithan, R. Raj, P. Prakash, A. Santosh, V. Theertha et al, "Green synthesis of silver nanoparticles from Justicia adhatoda plant extract with its diverse properties", *Journal of Physics: Conference Series, First International Conference on Advances in Physical Sciences and Materials*, vol.1706,p 012012, 2020. DOI:[10.1088/1742-6596/1706/1/012012](https://doi.org/10.1088/1742-6596/1706/1/012012).
- 17- I. Hussain, N. Singh, A. Singh, H. Singh and S. Singh, "Green synthesis of nanoparticles and its potential application", *Biotechnology Letters*, vol. 38, no. 4, pp.545-560, 2015. Available: [10.1007/s10529-015-2026-7](https://doi.org/10.1007/s10529-015-2026-7).
- 18- S. Mohamed, K. El-Naggar, M. Khalil, "Green Synthesis of Silver Nanoparticles using Egyptian Propolis Extract and its Antimicrobial Activity", *Egyptian Journal of Chemistry*, vol.65, no.7, pp.453-464, 2022. DOI: [10.21608/ejchem.2021.104296.4838](https://doi.org/10.21608/ejchem.2021.104296.4838)
- 19- A. Biswas, C. Vanlalveni, P. Adhikari, R. Lalfakzuala and L. Rokhum, "Green biosynthesis, characterization and antimicrobial activities of silver nanoparticles using fruit extract of Solanum viarum", *IET nanobiotechnology*, vol.127, pp. 933-938, 2018. Available: [10.1049/iet-nbt.2018.0050](https://doi.org/10.1049/iet-nbt.2018.0050)
- 20-(a) A. A. Moosa, A. M. Ridha, M. Hameed Allawi, "Process parameters for green synthesis of silver nanoparticles using leaves extract of Aloe vera plant", *International Journal of Multidisciplinary and Current Research (IJMCR)*, vol.3, pp.966-975, 2015. (b) A. A. Moosa, Mousa Ridha, M. Hameed Allawi, "Green Synthesis of Silver Nanoparticles using Spent Tea Leaves Extract with Atomic Force Microscopy", *International Journal of Current Engineering and Technology* , vol. 5, no. 5, pp. 3233–3241, 2015. [Online]. Available: <http://inpressco.com/category/ijcet>
- 21- A. A. Moosa and M. F. Muhsen, "Ceramic Filters Impregnated with Silver Nanoparticles for Household Drinking Water Treatment", *American Journal of Materials Science*, vol. 7, no. 6, pp. 232–239, 2017, Available: [10.5923/j.materials.20170706.02](https://doi.org/10.5923/j.materials.20170706.02).
- 22-Y. Yi, C. Wang, X. Cheng, K. Yi, W. Huang and H. Yu, "Biosynthesis of Silver Nanoparticles by Conyza canadensis and Their Antifungal Activity against Bipolaris maydis", *Crystals*, vol. 11, no. 12, p. 1443, 2021. Available: [10.3390/cryst11121443](https://doi.org/10.3390/cryst11121443)
- 23- A. A. Moosa , Z. H. Mahdi , M. A. Mutar, "Preparation of Graphene Oxide from Expanded Graphite at Different Microwave Heating Times", *Journal Engineering Technological Science*, vol.53, no.3, 2021, 210305. DOI: <https://doi.org/10.5614/j.eng.technol.sci.2021.53.3.5>.



- 24- P. V. Thinh, T. D. Nguyen, N. T. Thuong, V. T. T. HO, B. T. P. Quynh, L. G. Bach, "Influence Factors of Exfoliation Synthesis Exfoliated Graphite from Vietnamese Natural Graphite Flakes Using Microwave Irradiation", *Solid State Phenomena*, vol.279, pp.230–234, 2018. <https://doi.org/10.4028/www.scientific.net/SSP.279.230>
- 25- Y. Çelik and A. Kurt, "Three dimensional porous Expanded Graphite/Silver Nanoparticles nanocomposite platform as a SERS substrate", *Applied Surface Science*, vol. 568, pp.150946, 2021. Available: 10.1016/j.apsusc.2021.
- 26- S. R. Dhakate, R. B. Mathur. S. Sharma, M. Borah, T. L. Dhama, "Influence of Expanded Graphite Particle Size on the Properties of Composite Bipolar Plates for Fuel Cell Application", *Energy & fuels*, vol.23, pp.934–941, 2009.
- 27- M. Preethika, D. N. Ramila, H. S. Brahmari, G. Mani, K. S. Ashok, "Recent Trends in the Applications of Thermally Expanded Graphite for Energy Storage and Sensors" – A Review, *Nanoscale Advances*, vol.3, pp.6294-6309, 2021. DOI: 10.1039/d1na00109d.
- 28- J. He, L. Song, H. Yang, X. Ren, L. Xing, "Preparation of Sulfur-Free Exfoliated Graphite by a Two-Step Intercalation Process and Its Application for Adsorption of Oils", *Journal of Chemistry*, Article ID 5824976, 8 pages, 2017. <https://doi.org/10.1155/2017/5824976>
- 29- Z. Ying, X. Lin, Y. Qi, J. Luo, "Preparation and characterization of low-temperature expandable graphite", *Materials Research Bulletin*, vol.43, no.10, pp.2677-2686, 2008.
- 30- K. C. Tsai, H. C. Kuan, H. W. Chou et al., "Preparation of expandable graphite using a hydrothermal method and flame-retardant properties of its halogen-free flame-retardant HDPE composites", *Journal of Polymer Research*, vol.18, pp. 483–488, 2011. <https://doi.org/10.1007/s10965-010-9440-2>.
- 31- P. Mulvaney, "Surface Plasmon Spectroscopy of Nanosized Metal Particles", *Langmuir*, vol.12, pp.788-800, 1996. <https://doi.org/10.1021/la9502711>
- 32- V. Singh, A. Shrivastava, N. Wahi, "Biosynthesis of silver nanoparticles by plants crude extracts and their characterization using UV, XRD, TEM and EDX", *African Journal of Biotechnology*, vol.14, no.33, pp.2554- 2567, 2015. DOI: [10.5897/AJB2015.14692](https://doi.org/10.5897/AJB2015.14692).
- 33- M. Venkatesham, D. Ayodhya, A. Madhusudhan, N. Veera Babu, G. Veerabhadram, "A novel green one-step synthesis of silver nanoparticles using chitosan: catalytic activity and antimicrobial studies", *Applied Nanoscience*, vol.4, pp.113-119, 2012.
- 34- M. S. El-Gamal, S. S. Salem, A. M. Abdo, "Biosynthesis, characterization, and antimicrobial activities of silver nanoparticles synthesized by endophytic *Streptomyces* sp", *Egyptian Journal Biotechnology*, vol.56, pp. 69-85, 2018.
- 35- R. Mani, P. Vijayakumar, T. S. Dhas, K. Velu, D. Inbakandan et al., "Synthesis of biogenic silver nanoparticles using butter fruit pulp extract and evaluation of their antibacterial activity against *Providencia vermicola* in Rohu", *Journal King Saud University- Science*, vol.34, p.101814, 2022. DOI: 10.1016/j.jksus.2021.101814.
- 36- A. Shojamoradi, H. Abolghasemi, M. Esmaili, M. Foroughi-Dahr, H. Fatoorechi, "Experimental studies on congo red adsorption by tea waste in the presence of silica and Fe<sub>2</sub>O<sub>3</sub> nanoparticles", *Journal of Petroleum Science and Technology*, vol.3, no.2, pp.25-34, 2013. <https://www.sid.ir/en/journal/ViewPaper.aspx?id=45881>
- 37-S. Hou et al., "Silver Nanoparticles-Loaded Exfoliated Graphite and Its Anti-Bacterial Performance", *Applied Sciences*, vol. 7, no. 8, p. 852, 2017. Available: 10.3390/app7080852.
- 38- H. Padalia, P. Moteriya, S. Chanda, "Green synthesis of silver nanoparticles from marigold flower and its synergistic antimicrobial potential", *Arabian journal of chemistry*, vol.8, no.5, pp.732-741, 2015. DOI:<https://doi.org/10.1016/j.arabjch.2014.11.015>
- 39- R. Devi, B. Batra, S. Lata, S. Yadav and C. Pundir, "A method for determination of xanthine in meat by amperometric biosensor based on silver nanoparticles/cysteine modified Au electrode", *Process Biochemistry*, vol.48, no. 2, pp.242-249, 2013. Available: 10.1016/j.procbio.2012.12.009.
- 40- M. Parveen, F. Ahmad, A. M. Malla, S. Azaz, "Microwave-assisted green synthesis of silver nanoparticles from *Fraxinus excelsior* leaf extract and its antioxidant assay", *Applied Nanoscience*, vol.6, pp. 267-276. 2015. <https://doi.org/10.1007/s13204-015-0433-1>
- 41- S. Palithya, S. A. Gaddam, S. V. Kotakadi, J. Penchalaneni, N. Golla, S. Krishna, C. V. Naidu, "Green synthesis of silver nanoparticles using flower extracts of *Aerva lanata* and their biomedical applications", *Particulate Science and Technology*, vol.40, no.1, pp.84-96. 2022. DOI: [10.1080/02726351.2021.1919259](https://doi.org/10.1080/02726351.2021.1919259).
- 42-T. Tsekeli, T. Sebokolodi, H. Karimi-Maleh and O. Arotiba, "A Silver-Loaded Exfoliated Graphite Nanocomposite Anti-Fouling Electrochemical Sensor for Bisphenol A in Thermal Paper Samples", *ACS Omega*, vol. 6, no. 14, pp. 9401-9409, 2021. Available: 10.1021/acsomega.0c05836.
- 43- B. K. Mehta, M. Chhajlani, B. D. Shrivastava, "Green synthesis of silver nanoparticles and their characterization by XRD", *IOP Conference Series:Journal of Physics:Conference Series*, vol. 836, p. 012050, 2017.
- 44- M. Vanaja, G. Annadurai, "Coleus aromaticus leaf extract mediated synthesis of silver nanoparticles and its bactericidal activity", *Applied nanoscience*, vol. 3, no.3, pp.217-223, 2013. DOI 10.1007/s13204-012-0121-9.
- 45- S. S. Shankar, A. Ahmad, M. Sastry, "Geranium leaf assisted biosynthesis of silver nanoparticles", *Biotechnology Progress*, vol.19, no.6, pp.1627-1631, 2003. DOI: 10.1021/bp034070w. PMID: 14656132. *Science and Technology*, 3(2), 25–34(2013). <https://www.sid.ir/en/journal/ViewPaper.aspx?id=45881>